

Velocity Modulation Spectroscopy of Ions

Serena K. Stephenson[†] and Richard J. Saykally^{*}

Department of Chemistry, University of California-Berkeley, Berkeley, California 94720

Received November 22, 2004

Contents

1. Introduction	1
2. Theoretical Background	2
2.1 Glow Discharge	2
2.2 Modulation	3
2.2.1 Doppler Shift	3
2.2.2 Line width	4
2.2.3 Modulation Index	5
3. History and New Developments	6
3.1 Fourier Transform Velocity Modulation	7
3.2 Double-Modulation Spectroscopy	7
3.3 Bidirectional Velocity Modulation	7
3.4 OH-MR-VMS	8
3.5 Terahertz Velocity Modulation	8
3.6 Millimeter Wave Velocity Modulation	9
4. Molecular Ions	9
5. Conclusions	13
6. Acknowledgment	14
7. References	14

1. Introduction

The study of molecular ions was greatly accelerated by Oka's¹ development of tunable infrared laser absorption spectroscopy of glow discharges in 1980 via his initial detection of the vibrational spectrum of H_3^+ . Other important developments occurring concurrently with the tunable infrared absorption studies included work on infrared emission spectra in hollow cathode lamps² and infrared laser ion beam spectroscopy.³ Nevertheless, it remained very difficult to study spectra of more complex ions because of the overwhelming interference engendered by the presence of neutral absorbers, which are typically several orders of magnitude more abundant in discharge plasmas than are the ions themselves.

This obstacle was overcome in 1984 with the introduction of the velocity modulation technique.⁴ Soon after the initial study of HCO^+ , HNN^+ , H_3O^+ , and NH_4^+ , many other chemically important molecular cations were measured and spectroscopically characterized for the first time in work from several research groups.⁵ In 1985, velocity modulation was employed for the first successful detection of direct

absorption spectra of molecular anions by Owrutsky et al.⁶ In this initial study of the hydroxide ion (OH^-), the ability of velocity modulation detection not only to suppress the absorption features of neutral species but also to discriminate and label the respective absorptions of cationic and anionic species was demonstrated. This subsequently led to the characterization of many textbook anions, including N_3^- , NCO^- , NCS^- , NH_2^- , and FHF^- .⁷

One notable aspect of this work is that the relatively weak ion spectra could be extracted and identified reliably from simple absorption spectra of chemically complex discharge plasmas, without any mass selection. This was made possible by the effective suppression of neutral molecule absorptions, the labeling of ionic charge (+ or -) by the phase of the derivative-like line shape, the rough identification of carrier mass via the Doppler line width (approximately inversely proportional to the square root of reduced mass of the ion-buffer gas complex), and the very high spectral resolution (ca. 1×10^{-6} or 300 MHz) effected by velocity modulation spectroscopy.⁸ The spectroscopic technique itself is complemented and empowered by the impressive accuracy and generality of modern *ab initio* calculations⁹ of molecular ion structures and properties.

Since the initial development of velocity modulation² during the early 1980s, many other groups have adopted the technique, and several modifications and extensions have been made. One review, covering general advances in infrared laser absorption spectroscopy, was written in 1987 by Sears.¹⁰ A paper (written in Chinese) was published by Gao et al.¹¹ covering properties of velocity modulation such as the effects of discharge current, gas pressure, and pump velocity on spectral intensity. An overview of velocity modulation spectroscopy is presented here, covering both the basic theory, as well as recent developments. These include velocity modulation Fourier transform spectroscopy,¹² double modulation spectroscopy,¹³ bidirectional velocity modulation,¹⁴ enhancement by the heterodyne detection and the application of a magnetic field surrounding the discharge cell,^{15,16} and the extensions of velocity modulation to the terahertz regime¹⁷⁻¹⁹ as well as to the submillimeter frequency range.^{20,21} Finally, a complete summary of all ions observed using velocity modulation over the years is presented, including their respective transition frequencies and references in which they can be found.

* Corresponding author: Department of Chemistry, UC-Berkeley, Berkeley, CA 94720. Phone: (510) 642-8269. Fax: (510) 642-8369. E-mail: saykally@uclink4.berkeley.edu.

[†] Current address: ARS-USDA, Albany, CA 94710.



Dr. Serena K. Stephenson received her B. A. in chemistry from Carleton College in 1998. She then began graduate school in chemistry at the University of California at Berkeley under the direction of Prof. Richard Saykally and received her Ph.D. in 2003. The major focus of her dissertation was high-resolution terahertz spectroscopy of neutral water clusters and molecular ions. She is currently a chemist in the Bioproduct Chemistry and Engineering unit of the United States Department of Agriculture located in Albany, CA. She is researching processes for separating small alcohols from aqueous solutions.



Born in Rhinelander, Wisconsin, and educated at UW-Eau Claire and UW-Madison, Saykally has been a professor at the University of California-Berkeley since 1979. He and his students pioneered important advances in laser spectroscopy, including velocity modulation spectroscopy of ions, terahertz laser vibration-rotation-tunneling spectroscopy of clusters, infrared photon counting spectroscopy, and cavity ringdown spectroscopy. These have permitted the first detailed study of important textbook molecules, including the hydronium (H_3O^+) and hydroxide (OH^-) and ammonium (NH_4^+) ions, small water clusters, and carbon clusters. His recent work includes the spectroscopic determination of a universal water force field, the development of femtosecond nonlinear optical molecular imaging methods, and X-ray spectroscopy of liquid surfaces. A coauthor of over 300 publications, the recipient of over 35 honors and awards, Saykally is a member of the National Academy of Sciences and the American Academy of Arts and Sciences, and has recently received the Langmuir Prize in Chemical Physics from the American Chemical Society, the Centenary Medal of the UK Royal Society of Chemistry, and the E. O. Lawrence Award in Chemistry from the U.S. Department of Energy. He is an UC-Berkeley Distinguished Teacher and has been active at the national level in science education. Over 100 students and postdoctorals have trained in his research group. Saykally currently holds the Class of 1932 Distinguished Chair in the Department of Chemistry.

2. Theoretical Background

Velocity modulation spectroscopy is based on the following principles:

(1) Ions are produced with sufficient density ($> 10^9 \text{ cm}^{-3}$) in positive column discharge plasmas to permit direct detection of their IR absorption spectra.

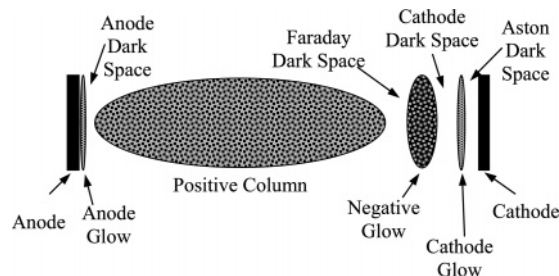


Figure 1. Shows the regions of a DC glow discharge occurring between the two electrodes.

(2) Ions are accelerated to average drift velocities that are comparable to their isotropic thermal velocity by the axial electric field ($\sim 10 \text{ eV/cm}$) of the plasma. This gives rise to Doppler shifts in ionic transitions that are of a similar magnitude as the associated Doppler widths ($\sim 1 \times 10^{-6}$).

(3) Neutral species are ordinarily not significantly affected by the plasma fields, either directly (Stark effects) or indirectly (electrophoresis effects). However, in some cases, neutrals that have undergone charge exchange can be observed using velocity modulation and Doppler shift concepts. Such is the case with metastable helium.²²

(4) By rapidly reversing the polarity of a DC positive column plasma, ionic transitions can be selectively detected with high sensitivity (1 part in 10^6) with phase sensitive electronics as a result of (1) and (2) above.

(5) Because of the anticorrelated translational motion of positive and negative ions in the plasma, phase sensitive detection unambiguously labels the sign of the charge on the carrier.

(6) Because both the frequency shift and the Doppler width of an ionic transition depend on the mass of the ion, the effective line width provides a crude measure of the mass of the absorber.

(7) Because the discharge is effectively shut off twice during each cycle of the driving field, absorptions of neutral molecules are “concentration modulated” at $2f$, yielding an absorption sensitivity comparable to that of velocity modulation itself.

2.1 Glow Discharge

For the purpose of describing the essential features of the plasma used in velocity modulation spectroscopy, one can assume that the discharge is established on a time scale much shorter than the switching rate, typically, $\leq 30 \text{ kHz}$. Therefore, a stable “DC” glow occurs on each half-cycle, with the difference between the two-half-cycles ideally being only the direction of the electric field. This implies that it is reasonable to discuss the different regions of a DC glow discharge (Figure 1) to understand the stable AC plasma.^{23,24} Under normal operating conditions the positive column occupies nearly all the space between the anode and the cathode, and this is the region of interest. Several characteristics make the positive column unique in the plasma. The main one exploited by velocity modulation is its homogeneity; that is, it exhibits a constant axial electric field and current density. Second, the principal mecha-

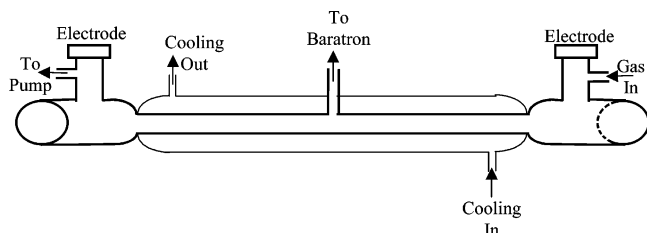


Figure 2. A diagram of the AC glow discharge cell showing the electrode location, cooling jacket, gas inlet/outlet ports, and the connection to the Baratron pressure gauge.

nism for the loss of positive ions is ambipolar diffusion of the ions and electrons to the cell walls, resulting in wall recombination, rather than by collisions with electrons in the plasma itself. This generates a nonuniform radial electric field, ordinarily of 1–10 V/cm, within the cell. The positive column typically has a relatively low, but constant, axial electric field of between 5 and 15 V/cm. By comparison, the negative glow has an extremely low electric field, on the order of a few tenths of a volt/cm, and the cathode dark space has a large electric field, ~ 1 kV/cm. From the cathode until the beginning of the positive column, there are large variations in electron energy and electric field, as well as ion and current densities. However, the design used in most velocity modulation cells (Figure 2) places the electrodes and these regions outside of the laser path. It is necessary to ensure that the glow discharge remains in a stable regime over a large range of conditions. In other words, the overall resistance of the discharge must remain positive. This is achieved by placing a ballast resistor in series with the output of the step-up transformer and the “hot” electrode, and for our system this is simply a 1 k Ω power resistor.

2.2 Modulation

The two central concepts underlying the mathematical description of velocity modulation are the line width of the relevant spectroscopic transition and the Doppler shift effected by the plasma electric field. Together, they determine the modulation depth, defined as (shift/width). Most velocity modulation studies have been performed in the infrared or visible regions wherein the primary contribution to the line width is Doppler broadening. However, in the few studies carried out in the terahertz region, the pressure broadening mechanism becomes a significant, if not *the* dominant, factor that determines the line shape.

2.2.1 Doppler Shift

A Doppler shift in the ion transition frequency results from the acceleration of ions by the axial component of the plasma electric field. This shift depends on the frequency of the transition, the magnitude of the field, the overall pressure and temperature in the plasma, and the mass and the polarizability of the plasma buffer gas. All of these are implicitly included in the following equation, which gives the first-order Doppler shift of an ion

in a positive column plasma:⁴

$$\delta\nu = \nu_0 \left(\frac{v_{\text{da}}}{c} \right) \quad (1)$$

where $\delta\nu$ is the Doppler shift, ν_0 is the center frequency of the transition, c is the speed of light (cm/s), and v_{da} is the axial drift velocity (cm/s) of the ion in the plasma. The axial drift velocity itself contains much information. It is defined as

$$v_{\text{da}} = KE \quad (2)$$

with K being the ion mobility (cm²/V s) and E being the electric field (V/cm). Magnitudes of the axial electric field in DC glow discharges are reported in the literature as generally between 5 and 15 V/cm, depending on the buffer gas properties, the diameter of the cell, and the total pressure.

Most ion mobility values listed in the literature are in the form of the reduced mobility (K_0), which allows values to be compared among different experiments. The mobility and the reduced mobility are related by

$$K = K_0 \left[\frac{760}{P(\text{Torr})} \right] \left[\frac{T_{\text{neut}}(\text{Kelvin})}{273.15} \right] \quad (3)$$

where P is the total pressure and T_{neut} is the translational temperature of the neutral atoms or molecules within the plasma. T_{neut} values are generally reported to be on the order of 200–800 K above the wall temperature, but there is a temperature gradient from the walls to the center of the cell, implying that the definition of a single neutral temperature for the cell is somewhat misleading. The translational and rotational temperatures are usually not completely equilibrated. There are two reasonable methods of determining the T_{neut} of a given plasma. The first is by measuring and fitting the concentration-modulated spectra of a neutral molecule to determine the Doppler-broadened line width and subsequently, the temperature. In this case, T is the neutral translational temperature. The second method is to measure the intensities of a series of rotational transitions for a molecule and then fit them using the Boltzmann relationship.

Mobilities of many ions have been measured by ion drift tube mass spectrometers, and the Langevin formula, as given by Mason and McDaniel,²⁷

$$K_0 = \frac{13.876}{\sqrt{\alpha\mu}} \quad (4)$$

provides a good method of calculating the reduced mobility. Here, α (\AA^3) is the dipolar–polarizability of the neutral collision partner, and μ (amu) is the reduced mass of the ion–neutral collision pair. This includes only the ion-induced dipole interaction, neglecting higher order terms. The mobility is a measure of how easily an ion can move through a given medium. The larger the polarizability of the neutral the more likely it will be to interact with the ion, slowing it down. Collision partners with high reduced mass are more likely to interact with each other, producing the same effect as increasing polar-

izability. Many experiments have been done over the years measure ion mobilities. A couple of typical ones that the interested reader can look to for a more complete treatment of mobilities are by Haese and Oka²⁵ and Picque.²⁶

One other note about using mobilities in the calculation of the Doppler shift is that experiments often employ a mixture of neutral gases, with different polarizabilities and reduced masses, composing the bulk of the buffer gas. In this case, a type of weighted average of the mobilities of the individual constituents can be used following Blanc's Law.²⁷

$$\frac{1}{K_{\text{mix}}} = \frac{\chi_1}{K_1} + \frac{\chi_2}{K_2} + \dots \quad (5)$$

where χ is the mole fraction of a given species in the neutral buffer gas and K is its corresponding mobility.

2.2.2 Line width

The modulation depth (shift/width) is the crucial parameter in velocity modulation spectroscopy, and over most of the electromagnetic spectrum, the shift and the width scale together, causing the modulation depth to be constant. With the exception of published studies done by K. Takagi,^{17,18,28} recent work by Stephenson and Saykally¹⁹ and the recently published studies by Savage et al. in the submillimeter region,^{20,21} all velocity modulation experiments have been done above 370 cm^{-1} , where the primary line broadening mechanism is Doppler broadening since this is proportional to frequency. Rigorously, the total peak width $\Delta\nu_{\text{tot}}$ reflects a convolution of the Gaussian (Doppler) and Lorentzian (pressure) line shapes. In some cases, such as in the occurrence of predissociation, the natural line width could also contribute to the total width. The width (HWHM) due to Doppler broadening is labeled $\Delta\nu_{\text{D}}$ and the pressure broadened width is $\Delta\nu_{\text{P}}$. In most spectroscopic studies, $\Delta\nu_{\text{D}} \gg \Delta\nu_{\text{P}}$ for the pressures attainable in AC glow discharges, meaning that $\Delta\nu_{\text{tot}} \approx \Delta\nu_{\text{D}}$. Only at frequencies below 200 cm^{-1} does the pressure broadening become important, and it is likely that it does not begin to dominate until $\sim 50 \text{ cm}^{-1}$, depending on the specific ion and buffer gas combination.

The Doppler width of a transition depends primarily on the randomized component of the drift velocity of the ion. The directional portion of the ion drift velocity is manifested in the Doppler shift discussed above, while the randomized part manifests itself as the Doppler width (HWHM) according to

$$\Delta\nu_{\text{D}} \cong 3.581 \times 10^{-7} v_0 \left[\frac{T_{\text{eff}}(\text{Kelvin})}{m(\text{amu})} \right]^{1/2} \quad (6)$$

where v_0 is the transition frequency, T_{eff} is the "effective ion translational temperature" in Kelvin and m is the ion mass in amu. Using T_{eff} rather than the actual temperature T_{neut} incorporates the randomized part of the drift velocity, and the equation for T_{eff} , given by Mason and McDaniel,²⁷ incorporates the mass of the buffer gas. If the ion temperature

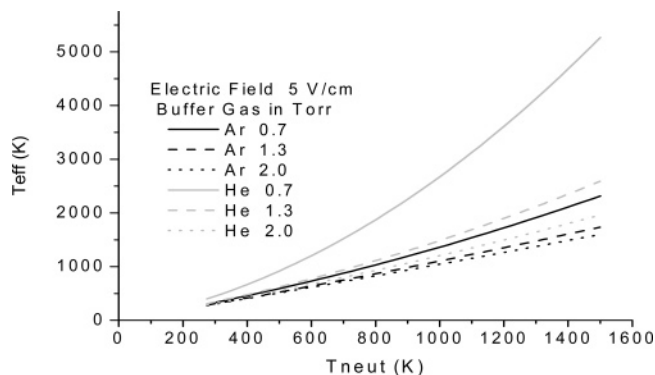


Figure 3. Calculation of sample T_{eff} values for ArH^+ throughout a range of possible neutral temperatures for both Ar and He buffer gases at 0.7, 1.3, and 2.0 Torr of total pressures using an electric field of 5 V/cm.

were identical to the buffer gas temperature, the reduced mass of the ion-neutral collision pair would be used in eq 6, instead of the ion mass. In general, if m (the mass of the ion) is approximately equal to M (the mass of the neutral), then the energy will be equally divided between the random and drift velocities. If $m \ll M$, then more energy is deposited in the random part, and if $m \gg M$ then it is mostly in the drift velocity, reflecting the fact that it is more difficult to make a heavy ion change direction if it is colliding with a light molecule. If a light ion accelerated by the field hits a heavy neutral atom, it is deflected more easily, randomizing its energy. The calculation of T_{eff} incorporates several assumptions, including that all ion-neutral collisions are elastic. The derivation of the total ion energy, described in detail by Mason and McDaniel,²⁷ yields:

$$\frac{3}{2}kT_{\text{eff}} = \frac{3}{2}kT_{\text{neut}} + \frac{1}{2}Mv_{\text{da}}^2 \quad (7)$$

This can be rearranged to give T_{eff} :

$$T_{\text{eff}} = T_{\text{neut}} + \frac{M}{3k}v_{\text{da}}^2 \quad (8)$$

with M being the mass (in kg) of the neutral, k being the Boltzmann constant (J/K) and v_{da} being the drift velocity. In addition to the axial drift field, there is also a radial field that results from the ambipolar diffusion of ions and electrons to the walls of the discharge tube, although it has no effect on the velocity modulation line shape. The radial field is governed by charge and mass balance equations related to the ambipolar diffusion of ions to the cell walls, and it is usually of about the same magnitude as the axial field. T_{eff} characterizes the total random energy of an ion, which contains two contributions, a genuine thermal part (T_{neut}) and a field part (containing v_{da}). Examples of T_{eff} versus T_{neut} , as calculated using eq 8, are shown in Figure 3. These are comparisons of T_{eff} to T_{neut} for ArH^+ in a glow discharge at three different total pressures of both Ar and He buffer gases (0.7, 1.3, and 2.0 Torr). For these examples, the simplification is made that the total cell pressure consists entirely of one specific buffer gas so Blanc's law does not need to be invoked

Table 1. Values Used in Calculations of Mobility and Broadening from Atkins²⁹ and Harris³⁰

	α (\AA^3)	mass (kg)
Ar	1.66	6.634×10^{-26}
He	0.20	6.646×10^{-27}
H ₂	0.819	3.347×10^{-27}

in the mobility calculation, but it should be kept in mind that, experimentally, this is unrealistic.

Minimizing the T_{eff} value is one way of increasing the modulation depth of an ion because of the effect of decreasing the Doppler width. It is useful to make some observations about the behavior of T_{eff} in light of Figure 3. The first is that using He as a buffer gas results in a larger T_{eff} due to the higher mobility of ArH⁺. The high mobility is a result of the low polarizability (α) of He, which decreases the interactions, resulting in unhindered ion movement through the buffer gas. Table 1 shows the values of polarizabilities and masses used making Figure 3. These are as reported in Atkins²⁹ and Harris.³⁰ A second observation is that, for a given T_{neut} , T_{eff} decreases significantly as the pressure in the cell increases, and this effect is much more pronounced for He than it is for Ar. It shows a major effect of the buffer gas pressure on the effective ion temperature, resulting in a pressure dependence of the Doppler width.

This is an unfortunate result when contemplating the extension of velocity modulation to the terahertz region. At low frequencies wherein Doppler broadening dominates, operation at lower pressures becomes critical. Here we see, however, that at low pressures the ion temperature is larger resulting in larger Doppler widths. When performing velocity modulation experiments below 100 cm^{-1} , it becomes a unique challenge to maintain a modulation depth of at least 1. The indirect dependence of the Doppler width on pressure complicates a direct and quantitative study of pressure broadening with velocity modulation in the terahertz region.

2.2.3 Modulation Index

Velocity modulation is essentially a form of frequency modulation caused by the Doppler shifting of an absorption in and out of resonance with the laser frequency. In the laboratory frame of reference, the ion population shifts according to the direction of the electric field, but in the rest frame of the ion, the light is being frequency modulated. To a good approximation, the lock-in amplifier acts as a Fourier filter, taking a modulated signal that contains two absorption profiles, one for the positive half of the discharge cycle, and one for the negative half. The two profiles are separated from each other by $2\delta v$, and when subtracted from each other, the resultant profile is the commonly observed first derivative shape. It should be noted, however, that if the two halves of the discharge are not symmetric, due to pressure gradients or electrode characteristics, then the resultant peak shape will be asymmetric, and absorptions of neutral species may not be completely eliminated from the spectra.

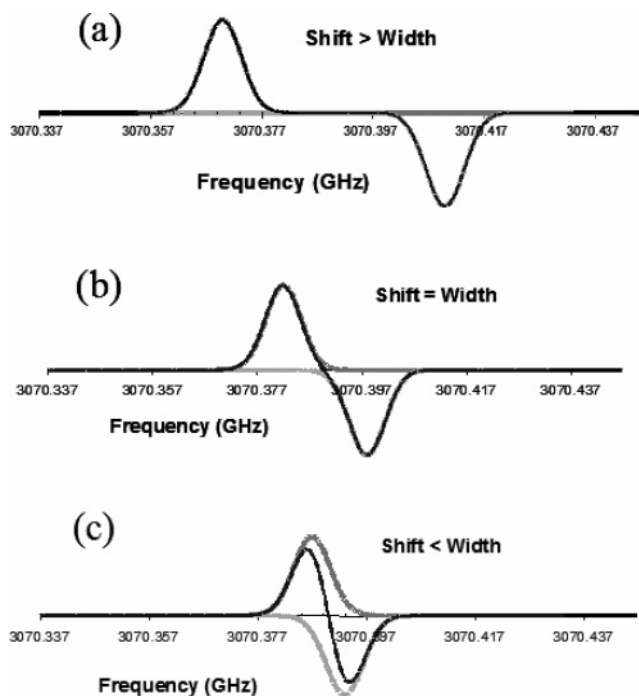


Figure 4. The black line in each of these is the sum of the two Doppler shifted peaks. The gray lines indicate the peak from each half-cycle of the discharge for varying shifts. (a) Modulation depth of 2.5; (b) modulation depth of 1; (c) modulation depth of 0.375.

The velocity modulated line shape depends explicitly on the modulation depth, $(\delta v/\Delta v_{\text{tot}})$. Here, δv is the Doppler shift, and Δv_{tot} is the half-width of the transition. In general, if $\delta v/\Delta v_{\text{tot}} > 1$ then the ions will be sufficiently modulated (the large modulation limit). If $\delta v/\Delta v_{\text{tot}} \approx 1$ velocity modulation can still be successful, but when $\delta v/\Delta v_{\text{tot}} < 1$ (small modulation limit) then ion signal intensity is lost from the overlap of the peaks generated in the two halves of the discharge cycle. The small modulation limit does not necessarily preclude the use of VM spectroscopy, but it does decrease the S/N. It is the small achievable modulation depth that poses the largest challenge to extending velocity modulation to frequencies below 100 cm^{-1} . Small changes in the plasma conditions, effecting total pressure, T_{neut} , T_{eff} , or buffer gas composition could significantly diminish the sensitivity. Figure 4 shows an example with three different modulation depths (2.5, 1, and 0.375) as calculated for the terahertz transition of ArH⁺ ($J = 5 \leftarrow 4$) reported by Stephenson and Saykally.¹⁹ It includes the peaks from both halves of the discharge cycle as well as the resultant 1f peak profile (i.e., the profile obtained by locking in to the plasma frequency itself). This figure is, in fact, only a qualitative illustration of the effect of modulation depth on the peak profile, assuming a square-wave velocity modulation. Rigorously, the 1f peak shape achieved by velocity modulation is the integral of the first Fourier component of the signal entering the lock-in amplifier.

Detailed calculations of velocity modulation line shapes using both square-wave and sine-wave modulation were performed by Farley who presented a very thorough discussion of line shapes in 1991.³¹ He uses the frequency distribution of the ions tracking with the modulation of the electric field. This fre-

quency distribution is given by

$$f(\omega) = \rho(t) \exp\left\{-\frac{[\omega - \omega_0 - \Omega_M \cos \omega_M t]^2}{2\Omega_D^2}\right\} \quad (9)$$

where $\rho(t)$ is the density of the ions with respect to time, ω is the frequency, ω_0 is the rest frequency of the transition, ω_M is the modulation frequency, Ω_M is the Doppler shift, and Ω_D is the zero-field Doppler width of the transition.³¹ The difference in the treatment of square-wave and sine-wave modulations lies in the definition of $\rho(t)$. For square-wave modulation the density is defined as

$$\rho(t) = \rho_0 q(r, \omega_M t) \quad (10)$$

where ρ_0 is the maximum density value and $q(r, \omega_M t)$ is the square-wave function. For a square wave modulation, the ion density tracks with the square wave function. Likewise, in sine-wave modulation, the ion density tracks with a sinusoidal function:

$$\rho(t) = \rho_0 |\cos(\omega_M t)| \quad (11)$$

The question becomes which of these two definitions of the change in ion density over time best describes what is actually happening within the plasma. It has been proposed that in low-frequency discharges (i.e., a couple of kilohertz) the square-wave is a reasonable description, but as higher frequencies are used in the plasmas, the sine-wave modulation becomes a more apt picture.³¹

Using the square-wave definition for the change of ion density, the first derivative velocity modulation line shape is

$$S_f = -\left(\frac{I_0 A_0}{2\pi}\right) 2 \sin\left(\frac{r\pi}{2}\right) \times \left[\exp\left\{-\frac{\left(\left(\frac{\omega - \omega_0}{\Omega_D}\right) - M\right)^2}{2}\right\} - \exp\left\{-\frac{\left(\left(\frac{\omega - \omega_0}{\Omega_D}\right) + M\right)^2}{2}\right\} \right] \quad (12)$$

where A_0 is the maximum value of the absorption, I_0 is the maximum laser intensity, ω_M is the discharge frequency, ω_0 is the transition frequency, ω is the laser frequency, and M is the modulation index. In the formulation of Farley, the modulation index is Ω_M/Ω_D where Ω_M is exactly the Doppler shift δv as given by eq 1, and Ω_D is $\Delta v_D/1.175$ (at zero-field). This is essentially the same definition as the “modulation depth” used by Gudeman et al.⁴ The major difference being that the “modulation index” uses fwhm values, rather than the HWHM values of Gudeman et al. This is a trivial difference, so in qualitative discussions these terms will be used interchangeably. The distinction will be stated only when necessary. In square wave modulation, as the modulation index becomes large the ion spectra will consist of two Gaussian profiles of opposite sign symmetric around

the center frequency of the transition, as already shown and discussed in Figure 4.

For sine wave modulation, there is no simple closed form as there is for the square-wave. Instead, it is calculated by the numerical integration of

$$S_f = -\left(\frac{A_0 I_0}{2\pi}\right) \int_0^{2\pi} \cos \omega_M t |\cos \omega_M t| \times \exp\left\{-\frac{\left(\left(\frac{\omega - \omega_0}{\Omega_D}\right) - M \cos \omega_M t\right)^2}{2}\right\} dt \quad (13)$$

where A_0 is the maximum value of the absorption, I_0 is the maximum laser intensity, ω_M is the discharge frequency, t is the time, ω_0 is the transition frequency, ω is the laser frequency, and M is the modulation index.

Although eq 13 is the exact description of the peak profile, it is possible to develop approximate expressions for the small and large modulation limits of the sine-wave modulation. In the small modulation limit, eq 13 can be approximated as

$$S_f = \left(\frac{8\Omega_M(\omega - \omega_0)}{(\Omega_D)^2 3}\right) \exp\left(\frac{-(\omega - \omega_0)^2}{2(\Omega_D)^2}\right) \quad (14)$$

with parameters defined as they are for eq 13. The large modulation limit for the sinusoidal modulation case is difficult to approximate and is achieved by employing two separate approximations, one near the line center and one for the wings. The interested reader is referred to the article by Farley for more details.³¹ Given that the dependence of line shapes in velocity modulation on experimental variables is relatively complicated, it is often difficult to accurately extract both Doppler shift and Doppler width information from an observed transition to determine parameters such as the drift velocity and the effective ion temperature within the plasma. Experimental line shape studies have been carried out both by Civis,³² using ArH^+ as a test ion, and by Gao et al.,¹¹ using N_2^+ , to study the effects of various velocity modulation parameters on the resulting line shapes.

3. History and New Developments

The critical step, which laid the foundation for the development of velocity modulation spectroscopy, was the observation of a small Doppler shift in the $J = 1 \leftarrow 0$ rotational transition of HCO^+ by Woods et al. in 1975.³³ A series of further experiments along these lines confirmed that the ion drift velocity observed in a DC glow discharge results in a Doppler shift, which changes depending on the magnitude and direction of the axial electric field.³⁴ The ability to measure Doppler shifts with such a setup was initially extended in two directions. First, it was used to make ionic mobility measurements,³⁵ and second, it was used to discriminate between absorptions and, less commonly, emissions due to ionic or neutral species in the infrared region. Velocity modulation spectroscopy was the result of using the Doppler

shifts to “filter” out the unshifted signals from neutral species in glow discharge plasmas.

There have been four major extensions of the basic velocity modulation experiment presented by Gudemann et al.⁴ The first, by Martin and Guelachvili, was coupling velocity modulation with Fourier transform infrared emission spectroscopy.¹² Second, a method of using a double modulation scheme to remove the background signal in velocity modulation was developed by Lan et al.¹³ Bidirectional velocity modulation was also developed as a method of eliminating optical pickup.¹⁴ Fourth, a technique using a magnetic field surrounding the positive column has been used, by Ma, to enhance the sensitivity of the absorptions of paramagnetic ions.^{15,16} The fifth extension of velocity modulation, implemented by the Takagi group, was to the study HeH⁺ and NeH⁺ in the terahertz region.^{17,18,28} Recently, ArH⁺ and H₃O⁺ have also been studied in the terahertz region by Stephenson and Saykally with a setup very similar to those used at higher frequencies,¹⁹ showing the promise for extending velocity modulation below 100 cm⁻¹. Last, in the past year, velocity modulation has been successfully adapted for use in the submillimeter region (between ~150 and 600 GHz, or ~5–20 cm⁻¹) by the Ziurys group.^{20,21}

3.1 Fourier Transform Velocity Modulation

Fourier transform spectroscopy (FTS) has the advantage of wide and continuous spectral coverage at a resolution of ca. 0.005 cm⁻¹ with scanning rates that far exceed conventional laser absorption spectroscopies, although sacrificing considerable (ca. 100-fold) sensitivity. Because of its lower sensitivity, FTS has generally been applied to the study of neutral molecules that are easy to produce in high number densities. However, in the work by Martin et al.,¹² it was shown that ionic transitions could be observed when the interference from much more abundant neutrals is suppressed via velocity modulation. It should be noted, however, that this was achieved at the expense of the signal-to-noise ratio. This work was also the first demonstration of velocity modulation emission spectroscopy. Only a couple of other studies have been done using velocity modulation emission spectroscopy techniques. One is on the ArH⁺ ion, by Picque and Guelachvili,³⁶ and the other is on N₂⁺, by Fan and Hamilton.³⁷ The design incorporated a lens at the end of a positive column to focus the light into a Michelson interferometer. The interferogram from normal Fourier transform spectroscopy is given by

$$I(\Delta) = \int_{-\infty}^{\infty} B(\sigma) \cos(2\pi\sigma\Delta) d\sigma \quad (15)$$

where $B(\sigma)$ is the intensity of the source as a function of wavenumber and Δ is the path length difference in the interferometer. The typical mode of modulation is to change Δ , but it turns out that modulation can also be achieved by changing σ . This is accomplished by the Doppler shifting of ions, via the alternating electric field in velocity modulation. The resulting interferogram was demodulated at the discharge frequency and was successful in increasing the

number of ArH⁺ transitions observed near 4 μm by eliminating large obfuscating signals from neutral species, namely, Rydberg transitions of ArH and rovibrational transitions of CO.

3.2 Double-Modulation Spectroscopy

A major limitation of the original velocity modulation technique arises from electrical pickup in the detection electronics and plasma light emission varying at the discharge frequency. Although most of the electrical pickup problems can be solved by careful shielding and grounding of the electronics, “optical” pickup by the detector of the emission from the plasma is a more difficult problem. The largest portion of the emission signal from the positive column will be modulated at twice the discharge frequency (2f), but there is a component that arises from the asymmetry between the two halves of the discharge plasma that is at the plasma frequency itself (1f). Demodulation in this case results in a drifting background, which fluctuates over the course of several seconds to several minutes. This baseline drift can obscure the small ion peaks, thus limiting the achievable signal-to-noise ratio.

The double modulation technique, developed by Lan et al., is a method of discriminating against this optical “pickup” by employing two different simultaneous modulations, processed in series by two separate lock-in amplifiers.¹³ First, the light sent into the velocity modulation cell is amplitude modulated (with a chopper) at 37 Hz. The discharge is then modulated at 25 kHz. Given that these two frequencies are so different, it is possible to first demodulate at 25 kHz and then send the output from that lock-in into a second, which demodulates at the chopped frequency. Since the 1f emission from the plasma is only modulated at the plasma frequency, demodulating at the amplitude modulated frequency of the laser light eliminates the background drift due to emission. In tests of the P(1) transition of HeH⁺ at 2843.9 cm⁻¹, part of the fundamental band 1–0, an increase of S/N of 2–3 orders of magnitude was achieved.¹³ In fact, without the double modulation setup the noise and background fluctuation were about 3 orders of magnitude larger than the desired signal eliminating the possibility of making an observation.

3.3 Bidirectional Velocity Modulation

This technique, like double-modulation, is designed to significantly reduce optical pick-up. It was implemented by Bawendi et al.¹⁴ as an extension of the double beam subtraction method³⁸ used to remove laser noise. In the double beam subtraction, the infrared light was split into two beams. One passed through the discharge tube multiple times (unidirectionally), while the other went directly to the detector and was used for laser noise subtraction; however, it did not remove the optical pickup from the discharge. In the bidirectional scheme, the laser beam is still split into two, but both beams pass unidirectionally through the cell multiple times in opposite directions. This serves to eliminate both laser noise and optical pick-up that occurs within the discharge.

It also effectively doubles the achieved signal-to-noise ratio due to the longer absorption path length.

3.4 OH-MR-VMS

In 1999 optical heterodyne magnetic rotation enhanced velocity modulation spectroscopy (OH-MR-VMS) was presented as a zero-background technique, applicable only to paramagnetic species, used to eliminate the large background fluctuations present in laser sources generally used for visible spectroscopy^{15,16} as well as the detector pickup of the plasma emission. Pure optical heterodyne velocity modulation has also been used³⁹ and has the advantage of being generally applicable to all ions. Recently, a paper has been published, in Chinese, which presents a general description of optical heterodyne velocity modulation in general.⁴⁰

The magnetic rotation enhancement aspect of the OH-MR-VMS technique is a result of the Faraday effect occurring in the interaction between polarized light and transition moments of paramagnetic molecules. This is also commonly called the magneto-optical effect. In the presence of a magnetic field, the polarization of incident light is changed by a dipole-allowed molecular transition. The amount of angle of rotation experienced by the polarized light is given by $\theta = VBl$. Here, θ (degrees) is the angle of rotation, V (degrees/Gauss cm) is the Verdet constant, B (Gauss) is the magnetic field, and l is the length, in cm, of the medium through which the light is traveling.^{41,42} The Verdet constant is determined experimentally and is different for each medium, or absorbing species, through which polarized light might travel. It can be measured by varying the magnetic field applied to a system and measuring the resultant angle of rotation. By including a set of polarizers, one before and one after the discharge cell, Wang et al. allowed only the light at the proper angle, i.e., with the proper polarization, to pass all the way to the detector.¹⁵ This was a form of double modulation, with the incoming light being polarization modulated at 480 MHz, and with plasma modulation occurring at 38 kHz.

The finding was that the intensity of the N_2^+ electronic spectra increased with increasing magnetic field strength, in agreement with previously observed behavior of the magnetic rotation effect for neutral paramagnetic species.^{43–46} In this particular case, however, there was another possible explanation for the enhancement, viz. that the magnetic field confines the electrons, increasing the plasma density.^{16,47} However, Luo et al.¹⁶ have shown that this confining effect results in only a small increase in sensitivity. Regardless of which mechanism made the biggest contribution to the signal increase, there was almost a 4-fold increase in S/N over the range from 100 to 500 G. This is a promising development for velocity modulation spectroscopy using intense laser sources with large background drifts. The major limitation to this technique is that the magneto-optical effect only applies to paramagnetic molecules.

Over the past five years, several studies have been performed using OH-MR-VMS at the Key Laboratory of Optical and Magnetic Resonance Spectroscopy at

East China Normal University in Shanghai. They presented a study of N_2^+ in their initial paper on this technique¹⁵ and a further study of it in 2001.⁴⁸ In addition Cl_2^+ , C_2^- , and CO^+ have all been measured in the range of 16700–17400 wavenumbers.^{43,49–51} Near-infrared spectra of $^{16}O_2^+$ between 12100 and 14100 cm^{-1} have been measured.^{52,53} Subbands of both H_2O^+ and D_2O^+ have also been measured in both the near-infrared and the visible regions,⁵⁴ and finally, the near-infrared spectrum of CS^+ has been obtained.^{55–58}

3.5 Terahertz Velocity Modulation

For many years, the velocity modulation technique was used only in frequency regions in which the origin of the line shape arises exclusively from Doppler broadening. However, in the terahertz region, both pressure broadening and the Doppler broadening mechanisms contribute to the total line shape and line width such that the assumption that both the line width and the Doppler shift are scaling the same frequency is no longer valid. Until the late 1990s, the lowest frequency velocity modulation experiment was the study of inversion motion in H_3O^+ at $\sim 370\text{ cm}^{-1}$ as reported in Liu et al.⁵⁹ In 1997 Matsushima et al.¹⁷ reported using velocity modulation coupled with the Tunable Far-Infrared spectrometer of Evenson and co-workers⁶⁰ to study the pure rotational spectra of HeH^+ and many of its isotopes between 2 and 5 terahertz ($60\text{--}170\text{ cm}^{-1}$). Previously, the pure rotation spectra for HeH^+ had been observed between 400 and 920 cm^{-1} .^{61,62} There had also been studies of the infrared rovibrational spectra.^{63,64} The terahertz laser system that they used generated the light by mixing two CO_2 laser beams on a MIM diode. From their work on HeH^+ , they determined the isotope independent Dunham parameters for HeH^+ .¹⁷ This study was accompanied by a series of other work on the pure rotational spectra of protonated noble gas atoms by looking at NeH^+ ,¹⁸ ArH^+ ,⁶⁵ and KrH^+ .⁶⁶ The velocity modulation technique was attempted for all of these species but used only for the HeH^+ and NeH^+ results. Only frequency modulation permitted the observation of KrH^+ , and it was stated that for ArH^+ , the results from frequency and velocity modulation were the same so they opted for using frequency modulation rather than velocity modulation for the published results.⁶⁵ Other velocity modulation results do exist for the ArH^+ in the infrared region.^{62,67}

Recently, ArH^+ and H_3O^+ have both been observed using velocity modulation between 60 and 105 cm^{-1} .¹⁹ This experiment was done with the Berkeley Terahertz spectrometer coupled with a water-cooled velocity modulation cell driven by a Plasmaloc 2 power supply. The $J = 5 \leftarrow 4$ ground-state rotational transition at 102 cm^{-1} has been observed with a S/N ratio of 770/1, which is at least an order of magnitude stronger than any other reported observation of this ion in the terahertz region, either by frequency modulation or velocity modulation.⁶⁸ The $J = 3 \leftarrow 2$ transition at 61.5 cm^{-1} was also observed with this set up but with a much smaller S/N ($\sim 15/1$), probably due to the Boltzmann population distribution of

states within the plasma. The $J_k = 7_5^+ \leftarrow 6_5^-$ of H_3O^+ was observed at 102 cm^{-1} as well,¹⁹ which is the first observation of a nonnoble gas complex via terahertz velocity modulation.

These studies demonstrate the feasibility of employing VM even under conditions wherein pressure broadening was previously thought to present an insurmountable obstacle to it. The terahertz region is a particularly important part of the spectrum for the study of ionic complexes; like the protonated water dimer⁶⁹ low-frequency librations and tunneling splittings can be measured and untangled, as for the cases of neutral water clusters.⁷⁰ The presence of an ion selective direct absorption technique in this region is potentially an important advance.

3.6 Millimeter Wave Velocity Modulation

Very recently, a study of SH^+ using velocity modulation in the submillimeter region was reported by the Ziurys group.²⁰ They also describe the measurement of CO^+ and HCO^+ with their more detailed discussion of the design of their millimeter/submillimeter velocity modulation spectrometer.²¹ Millimeter-wave light is generated by Gunn oscillators and coupled with Schottky diode multipliers to create light in the range of $\sim 2.2\text{--}22\text{ cm}^{-1}$. The biggest difference in the velocity modulation experiment in the millimeter wave region is that the inner diameter of the discharge cell is 10 cm, as compared to the 1–2 cm cells used for shorter wavelengths. The most obvious disadvantage of such large a diameter is that it produces a lower number density of ions. However, this cell diameter was necessary due to the large millimeter wave beam diameters. Teflon lenses were used at the beginning and the end of the 85-cm-long cell to help control the beam diameter and as the method of sealing the vacuum. Savage and Ziurys²¹ performed tests on both CO^+ and HCO^+ to demonstrate the technique at these low frequencies. Both of these ions had been studied previously, since they are both of major astronomical importance. CO^+ has been employed in plasma diagnostic studies^{51,71} and has been investigated by both vibrational⁷² and electronic⁵⁰ spectroscopies. HCO^+ was the first molecule to be studied by velocity modulation, with the spectrum of the ν_1 fundamental band⁷³ followed soon after by the bending mode⁷⁴ and hotbands.^{75,76} The extension of spectroscopic studies of these species to very low frequency is a powerful way to confirm and refine what is already known about the behavior of these ions. It has been thought that velocity modulation at very low frequencies would be ineffective since this is the range wherein pressure broadening dominates the line shape. As discussed above, at these very low frequencies, the Doppler shift may not be sufficient to compensate for the pressure-broadened width, which has minimal dependence upon frequency. To circumvent this problem, the Ziurys' group employed very low total pressures within the velocity modulation cell (40–50 mTorr). Instead of having the usual first-derivative transition profile, the blue-shifted portion of the peak (positive) was bigger than the red-shifted (negative) half by approximately a factor of 4. We note that this is similar

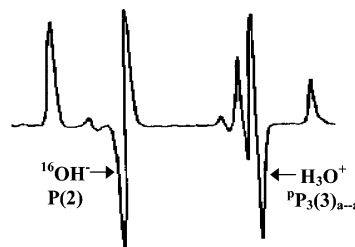


Figure 5. This is an example of the difference of phase between positive and negative ions that occurring in the 1f modulated signal as reported in Rosebaum et al. Reprinted with permission from ref 78. Copyright 1986 American Institute of Physics.

to the result effected by a pressure gradient in the cell. The other unusual result they encountered was a systematic shift of the center frequency of the velocity-modulated signal compared to the signal with source modulation.

Regardless of the idiosyncrasies of velocity modulation in the millimeter-wave region, it is clear that this technique nevertheless works at these low frequencies, and still allows for discrimination between transitions in neutral and ionic molecules. More accurate frequencies and additional transitions have now been measured for HCO^+ and CO^+ between 5.9 and 15.7 cm^{-1} .²¹ In addition, the $J = 1 \leftarrow 0$ transition of SH^+ has recently been observed.²⁰ The only other velocity modulation study of SH^+ was performed in the infrared.⁷⁷

4. Molecular Ions

A description of the original velocity modulation experiment was published in 1983 by Gudeman et al.⁴ Shortly afterward, several research groups exploited the new ability to perform ion-selective spectroscopy, resulting in the observation of the first infrared and electronic spectra of many textbook molecular ions. The initial burst of results came from the Saykally (Berkeley), Oka (Chicago), and Davies (Cambridge) groups through studies performed in the infrared and visible regions of the spectrum. Over the last two decades, numerous other research groups have joined in the search for ions using velocity modulation, and there has been a thorough line shape study performed by Farley, as discussed in the section on signal modulation.³¹ The present section describes all of the ion studies that have been made using velocity modulation. It should be noted again that this technique not only allows for the discrimination between ionic and neutral species, but also between ions of opposite charges. Figure 5 shows a comparison of the observed spectra of a negative ion ($^{16}\text{OH}^-$) and a positive one (H_3O^+) as reported in Rosenbaum et al.⁷⁸ Both positive and negative ions are included in Table 2, which gives a comprehensive list of the ions that have been studied to date using the velocity modulation technique. Far fewer anions have been studied than cations. Various isotopomers of the hydroxyl anion ($^{16}\text{OH}^-$, $^{18}\text{OH}^-$, and $^{16}\text{OD}^-$) were among the first.^{62,78–80} Also in the late 1980s NH_2^- , FHF^- , and ClHCl^- were observed by Tack et al.,⁸¹ Kawaguchi and Hirota⁸² and Kawaguchi,⁸³ respectively. More recently, Si_2^- has been observed by Liu

Table 2. Transitions, Frequencies, and References of Experiments Using Velocity Modulation in the Study of Both Positive and Negative Ions

ion	transition	study	frequency (cm ⁻¹)	reference
ArH ⁺ ArH ⁺ ArH ⁺ / ArD ⁺ ArH ⁺		ion mobility emission lf line shape		Haese and Oka (1983), ²⁵ Picque (1999) ²⁶ Picque and Guelachvili (1999) ³⁶ Civis (1994) ³²
	rotational transitions in $\nu = 0, 1, 2,$ 3, and 4		400–450	Liu et al. (1987) ⁶²
ArH ⁺	$J = 5 \leftarrow 4$ $J = 3 \leftarrow 2$		102.4 61.5	Stephenson and Saykally (2005) ¹⁹
³⁶ ArH ⁺ / ³⁸ ArH ⁺		rovibrational transitions	2500–2700	Filgueira et al. (1988) ⁶⁷
C ₂ ⁺	A ² Π _u – X ² Σ _g ⁺ (0,0) (1,1) (0,1)		3928.6595 3815.6264 2170.8479	Rehfuss et al. (1988) ¹⁴⁰
C ₂ ⁺	B ⁴ Σ _u ⁻ – X ⁴ Σ _g ⁻ (0,2) (1,3) (6,9)			Tarisitano et al. (2004) ¹⁴¹
C ₂ ⁻	B ² Σ _u ⁺ – X ² Σ _g ⁺	hot band transitions	16700–17400	Yu et al. (2003) ⁴³
CCl ⁺	$\omega_e = 1177.7196$	six lowest vibrational levels	1070–1210	Gruebele et al. (1986) ¹⁵⁶
CF ⁺	$\omega_e = 1792.6654$	seven lowest vibrational levels		Gruebele et al. (1986) ¹⁵⁸
CH ₃ ⁺ CH ₃ ⁺ CH ₂ D ⁺	ν_3 ν_1 fundamental ν_4 fundamental	> 1000 lines	2900–3300 3107.856 3004.765 3105.8406	Jagod et al. (1994) ¹⁴² Crofton et al. (1988), ³⁸ Crofton et al. (1985) ¹⁴³ Jagod et al. (1992), ¹⁴⁵ Rosslein et al. (1991) ¹⁴⁴
CHD ₂ ⁺ CH ₅ ⁺ C ₂ H ₂ ⁺ (DCCH ⁺) (¹³ C ₂ H ₂ ⁺) C ₂ H ₃ ⁺	ν_1 fundamental		3056.169	Jagod et al. (1992), ¹⁴⁵ Rosslein et al. (1991) ¹⁴⁴
C ₂ H ₂ ⁺ (DCCH ⁺) (¹³ C ₂ H ₂ ⁺) C ₂ H ₃ ⁺		infrared spectrum asymmetric hydrogen stretch	3135.901 3185.299 3128.389 3142.2	White et al. (1999) ¹³⁹ Jagod et al. (1992), ¹⁴⁶ Crofton et al. (1987) ¹⁴⁷
³⁵ ClH ³⁵ Cl ⁻ ³⁷ ClH ³⁷ Cl ⁻	ν_6		722.896 722.959	Crofton et al. (1989) ¹⁴⁸ Kawaguchi (1988) ⁸³
CO ⁺		plasma diagnosis		Yang et al. (2000), ⁵¹ Fan and Hamilton (1994) ⁷¹
CO ⁺	A ² Π ₁ – X ² Σ ⁺ (1,2) (2,3)		16700–17700	Zhuang et al. (2001) ⁵⁰
CO ⁺	X ² Σ ⁺	fundamental vibrational	2183.919	Davies and Rothwell (1985) ⁷²
CO ⁺	$J = 2 \leftarrow 1$ $J = 3 \leftarrow 2$ $J = 4 \leftarrow 3$ $J = 5 \leftarrow 4$	rotational transitions in X ² Σ	7.9 11.8 15.7 19.6	Savage et al. (in press) ²¹
CS ⁺	A ² Π – X ² Σ ⁺			Liu et al. (2001), ⁵⁶ Liu et al. (2002), ⁵⁷ Duan et al. (2003) ⁵⁸
CS ⁺	A ² Π – X ² Σ ⁺		12400–13000	Liu et al. (2000) ⁵⁵
Cl ₂ ⁺	A ² Π(u) – X ² Π(g)		16820–17350	Wu et al. (2005) ⁴⁹
FHF ⁻	ν_2 ν_3		1286.028 1331.150	Kawaguchi and Hirota (1987) ⁸²
H ₃ ⁺	ν_2	vibrational first overtone	3000–4200	Lindsay et al. (2001) ⁸⁸
H ₃ ⁺		review of all H ₃ ⁺ studies	<9000	Lindsay and McCall (2001) ⁸⁶
H ₃ ⁺		above barrier to linearity	>10000	Gottfried et al. (2003) ³⁹
H ₃ ⁺		destruction rate constant		Lindsay et al. (2000) ⁹⁵
H ₃ ⁺ H ₃ ⁺ H ₃ ⁺ H ₃ ⁺ H ₃ ⁺ H ₃ ⁺ H ₃ ⁺		rovibrational high rotational levels “forbidden” transitions	1.25 μm 2690–3580 3000–3200 4557–5094 6860–6925 6806–7266	McCall and Oka (2000) ⁹³ Uy et al. (1994) ⁹² Xu et al. (1992) ⁹⁴ Xu et al. (1990) ⁸⁹ Lee et al. (1991) ⁹⁰ Ventrudo et al. (1994) ⁹¹
H ₃ ⁺	2ν ₂ 3ν ₂ 3ν ₂	hotband transitions	2000–3000	Bawendi et al. (1990) ¹⁴

Table 2. (Continued)

ion	transition	study	frequency (cm ⁻¹)	reference
H ₃ ⁺	ν_2 fundamental		2521.30817	Watson et al. (1984) ⁸⁷
H ₂ D ⁺	ν_2 fundamental		2205.87	Foster et al. (1986) ⁹⁶
	ν_3 fundamental		2335.45	
HBBr ⁺			937.5696	Hunt et al. (1999) ¹⁵⁴
			936.0554	
HBCl ⁺	ν_3 fundamental		1105–1170	Hunt et al. (1999) ¹⁵⁵
HBr ⁺		fine and hyperfine splittings	1975–2360	Chanda et al. (1995) ¹⁵⁰
HCNH ⁺	ν_3 fundamental		2155.702	Liu et al. (1988) ¹³⁶
HCNH ⁺	ν_5 fundamental		645.9033	Ho et al. (1987) ¹³⁵
HCNH ⁺	ν_1	NH-stretch	3482.844	Altman et al. (1984), ¹³⁷ Altman et al. (1984) ¹³⁸
	ν_2	CH-stretch	3187.863	
HCO ⁺	00 ⁰⁰	fundamental	2183.95	
	00 ⁰¹	hotbands	2163.839	Liuet al. (1988), ⁷⁶ Davies et al. (1984) ⁷⁵
	01 ¹⁰		2187.0844	
HCO ⁺		bending mode	829.721	Davies and Rothwell (1984) ⁷⁴
HCO ⁺	ν_1 fundamental		3088.739	Amano (1983) ⁷³
HCO ⁺	$J = 2 \leftarrow 1$	rotational transitions in X ¹ Σ	5.95	Savage et al. (in press) ²¹
	$J = 3 \leftarrow 2$		8.92	
	$J = 4 \leftarrow 3$		11.89	
	$J = 5 \leftarrow 4$		14.86	
	$J = 6 \leftarrow 5$		17.84	
	$J = 6 \rightarrow 7$		20.81	
HCS ⁺	ν_1	rovibration	3141.682	Rosenbaum et al. (1985) ¹⁶⁷
H ³⁵ Cl ⁺	² $\Pi_{3/2}$		2500–2700	Davies et al. (1986) ¹⁴⁹
H ³⁷ Cl ⁺	² $\Pi_{1/2}$			
H ₂ F ⁺	ν_3	vibrational	3334.689	Schafer and Saykally (1984), ¹⁵²
	ν_1		3348.708	Schafer and Saykally (1984) ¹⁵³
HI ⁺	X ² Π	electronic state	2195.243	Chanda et al. (1995) ¹⁵¹
HN ₂ ⁺ / DN ₂ ⁺	ν_1 hotbands		2900–3500	Kabbadj et al. (1994), ¹²³ Owrutsky et al. (1986) ¹²⁴
DN ₂ ⁺	ν_1 fundamental bend-excited hotband		2618.774	Nesbitt et al. (1984) ¹²⁵
			2636.983	
D ₂ O ⁺	$\Sigma (0,9,0)-(0,0,0)$ $\Delta (0,9,0)-(0,0,0)$ $\Pi (0,8,0)-(0,0,0)$ $\Pi (0,10,0)-(0,0,0)$		16400–17600	Gan et al. (2004) ⁵⁴
H ₂ O ⁺	$\Sigma (0,7,0)-(0,0,0)$ $\Delta (0,7,0)-(0,0,0)$ $\Pi (0,6,0)-(0,0,0)$		12200–14000	
H ₂ O ⁺	$\Sigma (0,11,0)-(0,0,0)$ $\Delta (0,11,0)-(0,0,0)$		12000–13400	Huet et al. (1997) ¹¹⁴
H ₂ O ⁺	ν_1		16600–17600	Luo et al. (2001) ¹⁶ Wu et al. (2003) ¹¹⁵
H ₂ O ⁺	ν_3		3212.859	Huet et al. (1992) ¹¹²
H ₂ O ⁺	(0,7,0)-(0,0,0) (0,8,0)-(0,0,0)		3259.036	
H ₂ O ⁺			14794–15475	Das and Farley (1991) ¹¹³
H ₂ O ⁺			1431.198	Brown et al. (1989) ¹¹¹
H ₂ O ⁺	ν_3		3253.03	Dinelli et al. (1988) ¹¹⁰
H ₂ O ⁺			435–440	Liu et al. (1987) ⁶²
H ₃ O ⁺	ν_1 and ν_3 fundamentals		3300–3500	Tang and Oka (1999) ¹⁰³
H ₃ O ⁺	“forbidden” $\Delta(k-1) = 3$		3200–3500	Uy et al. (1997) (104)
H ₃ O ⁺	$(\nu_2 + \nu_3)^+ \leftarrow \nu_2^+$ $\nu_3^- \leftarrow 0^-$ $\nu_3^+ \leftarrow 0^+$		3549.953 3518.950 3535.562	Ho et al. (1991), ¹⁰⁵ Begemann and Saykally (1985), ⁹⁷ Begemann et al. (1983) ⁹⁸
H ₃ O ⁺	$1^- \leftarrow 1^+$	inversion	372.9	Liu and Oka (1985) ¹⁰⁰
H ₃ O ⁺	ν_3 a–a		3519.3953	Stahn et al. (1987) ¹⁰⁶
	ν_3 s–s		3535.9602	
H ₃ O ⁺	$\nu_2 (1^- \leftarrow 0^+)$ $\nu_2 (1^+ \leftarrow 0^-)$		954.4 525.829	Haese and Oka (1984), ⁹⁹ Davies et al. (1985), ¹⁰¹ Davies et al. (1984) ¹⁰²
H ₃ O ⁺	$7_5^+ \leftarrow 6_5^-$	ground-state inversion levels	102.7	Stephenson and Saykally (2005) ¹⁹
H ₃ ¹⁸ O ⁺	ν_2		942.77	Haese and Oka (1988) ¹⁰⁷
HeH ⁺		pure rotational	590–920	Liu and Davies (1997) ⁶¹
HeH ⁺	low J rotational transitions	several isotopic combinations	60–170	Matsushima et al. (1997) ¹⁷
HeH ⁺ / HeD ⁺	$\nu = 0$ through $\nu = 3$		1700–3300	Purder et al. (1992) ⁶³
HeH ⁺	$\nu = 1 \leftarrow 0$ $\nu = 2 \leftarrow 1$	several isotopic combinations	2300–3000	Crofton et al. (1989) ⁶⁴
HeH ⁺	$\nu = 0$ $J = 7 \leftarrow 6$		448.160	Liu et al. (1987) ⁶²

Table 2. (Continued)

ion	transition	study	frequency (cm^{-1})	reference
N_2^+	$J = 12 \leftarrow 11$ $\text{A}^2\Pi(\text{u}) \leftarrow \text{X}^2\Sigma(\text{g})^+$ (3,3) (4,4)		410.553 8119.7 7826.57	Tarsitano and Oka (2003) ¹¹⁶
N_2^+	$\text{A}^2\Pi(\text{u}) \leftarrow \text{X}^2\Sigma(\text{g})^+$ (2,0)			Gao et al. (2001) ¹¹
N_2^+	$\text{B}^2\Sigma(\text{u})^+ \leftarrow \text{X}^2\Sigma(\text{g})^+$ (2,0) (3,1) (14,1) (4,2) (5,3) (6,4) (7,5)		30000	Collet and Huet (1999), ¹¹⁹ Collet et al. (1998) ¹²⁰
N_2^+	$\text{A}^2\Pi(\text{u}) \leftarrow \text{X}^2\Sigma(\text{g})^+$ (6,3)	emission	13000–13700 UV and far-UV	Bachir et al. (1995) ¹¹⁷ Fan and Hamilton (1994) ³⁷
N_2^+	$\text{A}^2\Pi(\text{u}) \leftarrow \text{X}^2\Sigma(\text{g})^+$ (2,5)		2186.767	Ho et al. (1992) ¹¹⁸
N_2^+	$\text{A}^2\Pi(\text{u}) \leftarrow \text{X}^2\Sigma(\text{g})^+$ (11,5) (12,6)		16800–17573	Wu et al. (2001) ⁴⁸
$^{14}\text{N}^{15}\text{N}^+$	$\text{A}^2\Pi(\text{u}) \leftarrow \text{X}^2\Sigma(\text{g})^+$ (3,6)		2102.034	Ho et al. (1992) ¹¹⁸
NeH^+	$\nu = 0$ $J = 13 \leftarrow 12$		427.413	Liu et al (1987) ⁶²
NeH^+ / NeD^+		pure rotational	terahertz	Matsushima et al. (1998) ¹⁸
NH_2^+	ν_3	four hotbands	3359.932	Okumura et al. (1989) ¹²¹
NH_2^+	ν_1		2900–3500	Kabbadj et al. (1996) ¹²²
NH_2^-	ν_1		3121.931	Tack et al. (1986) ⁸¹
NH_2^-	ν_3		3190.291	
NH_3^+			2900–3500	Huet et al. (1994) ¹²⁶
NH_3^+	ν_3			Bawendi et al. (1989) ¹²⁷
NH_3^+	ν_1		903.3893	Lee and Oka (1991) ¹²⁸
NH_3^+	ν_2		939.771	
NH_4^+ / ND_4^+	ν_4		~2500	Crofton and Oka (1987) ¹²⁹
NH_4^+	ν_3		3343.139	Schafer et al. (1984), ¹³⁰ Crofton et al. (1983), ¹³¹ Schafer et al. (1983) ¹³²
NO^+		vibrational	2344.022	Ho et al. (1991) ¹³³
OH^+	ν_0	fundamental	2956.3698	Rehfuss et al. (1992), ¹⁰⁹ Crofton et al. (1985) ¹⁰⁸
OH^+	ν_1		2799.347	
OH^+	ν_2		2648.49	
OH^+	ν_3		2503.802	
OH^+	ν_4		2365.427	
OH^+		pure rotational	410–440	Liu et al. (1987) ⁶²
OH^-	$\nu = 0$ $J = 10 \leftarrow 9$ $J = 11 \leftarrow 10$		366.871 401.776	Liu et al (1987), ⁶² Liu and Oka (1986) ⁷⁹
$^{16}\text{OH}^-$		vibrational	3555.605	Rosenbaum et al. (1986) ⁷⁸
$^{18}\text{OH}^-$			3544.455	
OD^-		fundamental	2625.332	Rehfuss et al. (1986) ⁸⁰
O_2^+	$\text{A}^2\Pi_u - \text{X}^2\Pi_g$	rovibrational	12400–12700	Zheng et al. (2004) ⁵² Zheng et al. (2005) ⁵³ Civis et al. (1989) ⁷⁷
SH^+		$\omega_e = 2547.171$		
SH^+	$N = 1 \leftarrow 0, J = 2 \leftarrow 1$ $N = 1 \leftarrow 0, J = 1 \leftarrow 0$	hyperfine transitions in the $\text{X}^3\Sigma^-$ ground state	~17.5 ~11.5	Savage and Ziurys (2004) ²⁰
Si_2^-	$\text{A}^2\Pi(\text{u}) \leftarrow \text{X}^2\Sigma(\text{g})^+$ (1,0) (2,0)		670–810 1200–1340	Liu and Davies (1996) ⁸⁴
Si_2^-	$\text{A}^2\Pi(\text{u}1/2) \leftarrow \text{X}^2\Sigma(\text{g})^+$		740–820	Liu and Davies (1996) ⁸⁵
SiCl^+	fundamentals and hotbands	several isotopic combinations	630–7000	Fan et al. (1998) ¹⁵⁷
SiH^+	$\text{X}^1\Sigma^+$ fundamental		~2100	Davies and Martineau (1988) ¹⁶⁴
SiH_3^+	ν_2 fundamental ν_4 fundamental		838.067 938.397	Davies and Smith (1994), ¹⁶⁵ Smith et al. (1992) ¹⁶⁶
TiCl^+			17100–18600	Focsa et al. (1997) ¹⁵⁹
TiCl^+	[17.9] ³ $\Delta - \text{X}^3\Phi$ [17.9] ³ $\Delta - (1)^3\Delta$		17800–18500	Kaledin and Heaven (1997) ¹⁶⁰
TiCl^+	³ $\Delta(3d4s) - \text{X}^3\Phi(3d^2)$		17800–18300	Focsa et al. (1997) ¹⁶¹
TiF^+	[17.6] ³ $\Delta - \text{X}^3\Phi$		16800–18600	Focsa et al. (1998) ¹⁶²
TiF^+		electronic states		Focsa and Pinchemel (1999) ¹⁶³

and Davies,^{84,85} and C_2^- has been studied by Yu et al.⁴³

The ions in Table 2 are listed in alphabetical order. In cases in which the observed peaks have been assigned to specific rotational, vibrational, or electronic transitions, the assignments are presented as either specific band origins or frequency ranges over which the transitions were measured. When there are no specific assignments presented in the literature, some description of the type of study is given along with the frequency ranges. Many of these ions have been studied by other techniques as well, but it is outside of the scope of this review to include results obtained from those studies.

The two most heavily studied ions using velocity modulation are H_3^+ and H_3O^+ , together accounting for nearly 20% of total number of papers published. H_3^+ is a cation of major astrochemical importance and has been probed extensively throughout the infrared region. A good review of what is known about H_3^+ is described in the review by Lindsay and McCall.⁸⁶ The studies have ranged from the fundamental ν_2 band,⁸⁷ to the first,⁸⁸ second,⁸⁹ and third^{90,91} overtones of it. High rotational levels,⁹² the rovibrational spectrum,⁹³ hotband transitions,¹⁴ “forbidden” transitions,⁹⁴ and nonlinear configurations³⁹ have all been reported. In addition, the destruction rate constant has been measured.⁹⁵ Only one isotopic variant has been studied, and that is H_2D^+ by Foster et al.⁹⁶ The hydronium ion (H_3O^+) has also been the focus of many velocity modulation efforts particularly because of the fundamental interest of the inversion tunneling splittings. In fact, this ion was the focus of many studies in the first years by the Saykally group,^{97,98} the Oka group,^{99,100} and the Davies group.^{101,102} Since then, there have been several more studies of H_3O^+ in the infrared,^{103–106} and one in the far-infrared region.¹⁹ In addition, the ν_2 fundamental band of $H_3^{18}O^+$ has been observed.¹⁰⁷

Closely related to H_3O^+ are the H_2O^+ and OH^+ moieties, although it is evident that the plasma discharge conditions that optimize these later species are very different from those used to study H_3O^+ . For OH^+ , studies of the pure rotational⁶² and the rovibrational^{108,109} spectra have been published. H_2O^+ has been the focus of more studies, primarily because of its important roles in astronomy, atmospheric studies, and chemistry. Rotational,⁶² as well as rovibrational,^{110–112} spectra have been obtained throughout the infrared, and several studies of its electronic spectra have been done throughout the near-infrared^{154,113,114} and visible^{16,54,115} regions.

Velocity modulation has also been employed in the study of several nitrogen containing molecular ions. The most commonly studied of these is N_2^+ , especially the Meinel system ($A^2\Pi(u) \leftarrow X^2\Sigma(g)^+$). The Meinel system has been studied both by traditional velocity modulation techniques^{116–118} as well as by the recent optical heterodyne magnetic resonance velocity modulation technique^{11,48} discussed earlier in this review. Absorption transitions^{119,120} involving $B^2\Sigma(u)^+ \leftarrow X^2\Sigma(g)^+$ near 30 000 cm^{-1} as well as emission transitions in the UV and far-UV regions³⁷ have been measured. For NH_2^+ , the ν_3 fundamental band,¹²¹ as well as

hotbands¹²² have been reported. For HN_2^+ , and its isotopic variant (DN_2^+), both hotbands and fundamental bands have been observed using velocity modulation.^{123–125} In addition, the spectroscopies of NH_3^+ ,^{126–128} which has an inversion splitting analogous to H_3O^+ , and NH_4^+ ^{129–132} have both been studied with velocity modulation. The fundamental vibrational band of NO^+ ¹³³ has been measured, and studies of $HCNH^+$ have been performed. $HCNH^+$ is an ion of astronomical importance, especially as it relates to planetary science and the atmosphere of Titan, one of Saturn’s moons.¹³⁴ Several fundamental vibrational bands^{135,136} have been measured using VM, including the NH and CH stretching modes.^{137,138}

Several carbon and hydrocarbon cations have been measured as well. One of the most interesting results is the gas-phase infrared spectrum of the superacid species CH_5^+ . The nature of this molecule and the complexity of the tunneling which it exhibits have made assignment of observed transitions in the infrared spectrum impossible.¹³⁹ This ion would be of great interest to study in the terahertz region where low lying rotational levels and tunneling splittings may be able to be observed directly without the complications of perturbations due to vibrations. Transitions of $C_2^{+140,141}$ and C_2^- ⁴⁹ have been seen as well as the methyl cation^{38,142,143} and its deuterated forms.^{144,145} The asymmetric hydrogen stretch for $C_2H_2^+$, as well as $DCCH^+$ and $^{13}C_2H_2^+$, has been reported.^{146,147} Last, data have been obtained for $C_2H_3^+$.¹⁴⁸

A series of halogen halide ions, of interest because they tend to act as a halide atom perturbed by a neighboring proton, have been examined using velocity modulation. This series consists of HCl^+ ,¹⁴⁹ HBr^+ ,¹⁵⁰ and HI^+ .¹⁵¹ The similar ion, H_2F^+ , has also been studied.^{152,153} Also, similar, in that they are cations containing a halogen atom, are the velocity modulation studies on $HBBr^+$ ¹⁵⁴ and $HBCl^+$.¹⁵⁵ Halogen-containing cations of interest in semiconductor plasma etching process have also been measured using velocity modulation within the ac plasma. The three that have been studied are CCl^+ ,¹⁵⁶ $SiCl^+$,¹⁵⁷ and CF^+ .¹⁵⁸ Ions containing both a halogen atom and a transition metal atom are of potential interest in astrophysical studies and both $TiCl^+$ ^{159–161} and TiF^+ ^{162,163} have been examined by high-resolution spectroscopy for the first time using velocity modulation.

Finally, there are a few molecular ions for which velocity modulation has proved important to their study, which do not fit well in any of the preceding categories. The first, of possible interest in the interstellar medium, is the SiH^+ cation.¹⁶⁴ Second, of interest in plasma etching of silicon, is the SiH_3^+ ion.^{165,166} Last, the infrared rovibrational spectrum of HCS^+ has been reported.¹⁶⁷

5. Conclusions

Over the last two decades, velocity modulation techniques have been improved and extended to new frequency regions and applications. Improvements have been made in removing pickup noise and background signal drift that previously limited the

overall sensitivity. The spectral regions accessible by velocity modulation have also been shown to be more extensive than the early papers indicated. The small modulation limit is not necessarily prohibitive for the application of this technique, and velocity modulation has thus been extended to the terahertz region yielding S/N ratios an order of magnitude larger than previous studies of ions in this frequency range¹⁹ and has even been successfully demonstrated in the millimeter wave region.^{20,21} Optical heterodyne velocity modulation is becoming a prevalent technique for removing background noise from spectra, and the coupling of that with magnetic resonance spectroscopy has been, and will likely continue to be, very fruitful. Even though many molecular ions have already been observed with this technique, the continued improvements in both sensitivity and generality imply that it will be useful in the future study of many molecular ion systems.

6. Acknowledgment

This work was supported by the Experimental Physical Chemistry Program of the National Science Foundation.

7. References

- Oka, T. *Phys. Rev. Lett.* **1980**, *45*, 531.
- Brault, J. W.; Davis, S. P. *Phys. Scr.* **1982**, *25*, 268.
- Tolliver, D. E.; Kyrala, G. A.; Wing, W. H. *Phys. Rev. Lett.* **1979**, *43*, 1719.
- Gudeman, C. S.; Begemann, M. H.; Pfaff, J.; Saykally, R. J. *Phys. Rev. Lett.* **1983**, *50*, 727.
- Gudeman, C. S.; Saykally, R. J. *Annu. Rev. Phys. Chem.* **1984**, *35*, 387.
- Owrutsky, J. C.; Rosenbaum, N. H.; Tack, L. M.; Saykally, R. J. *J. Chem. Phys.* **1985**, *83*, 5338.
- Owrutsky, J.; Rosenbaum, N.; Tack, L.; Gruebele, M.; Polak, M.; Saykally, R. J. *Philos. Trans. R. Soc. London A* **1987**, *324*, 97.
- Saykally, R. J. *Science* **1988**, *239*, 157.
- Lee, T. J.; Schaefer, H. F. *J. Chem. Phys.* **1985**, *83*, 1784.
- Sears, T. J. *Faraday Trans. 2* **1987**, *83*, 111.
- Gao, H.; Liu, H. P.; Duan, C. X.; Lin, J. L.; Guo, Y. Q.; Liu, X. Y.; Huang, G. M.; Li, J. R.; Li, F. Y.; Liu, Y. Y. *Spectrosc. Spectral Anal.* **2001**, *21*, 279.
- Martin, P. A.; Guelachvili, G. *Phys. Rev. Lett.* **1990**, *65*, 2535.
- Lan, G.; Tholl, H. D.; Farley, J. W. *Rev. Sci. Instrum.* **1991**, *62*, 944.
- Bawendi, M. G.; Rehfuss, B. D.; Oka, T. *J. Chem. Phys.* **1990**, *93*, 6200.
- Wang, R. J.; Chen, Y.; Cai, P.; Lu, J.; Bi, Z.; Yang, X.; Ma, L. *Chem. Phys. Lett.* **1999**, *307*, 339.
- Luo, M.; Bi, Z.; Cai, P.; Wang, R.; Yang, X.; Chen, Y.; Ma, L. *Rev. Sci. Instrum.* **2001**, *72*, 2691.
- Matsushima, F.; Oka, T.; Takagi, K. *Phys. Rev. Lett.* **1997**, *78*, 1664.
- Matsushima, F.; Ohtaki, Y.; Torige, O.; Takagi, K. *J. Chem. Phys.* **1998**, *109*, 2242.
- Stephenson, S. K.; Saykally, R. J. *J. Mol. Spectrosc.* **2005**, *231*, 145.
- Savage, C.; Apponi, A. J.; Ziurys, L. M. *Astrophys. J.* **2004**, *608*, L73–L76.
- Savage, C.; Ziurys, L. M. *Rev. Sci. Instrum.* **2005**, *76*, 1.
- Suh, M. H.; Hong, X.; Miller, T. A. *Chem. Phys.* **1998**, *228*, 145.
- Llewellyn-Jones, F. *The Glow Discharge and an Introduction to Plasma Physics, Methuen's Monographs on Physical Subjects*; Wiley: New York, 1966.
- Radunsky, M. Ph.D. Thesis, University of California-Berkeley, 1989.
- Haese, N. N.; Oka, T. *Proc. Soc. Photo-Opt. Inst. Eng.* **1983**, *438*, 165.
- Picque, N. *Chem. Phys. Lett.* **1999**, *310*, 183.
- Mason, E. A.; McDaniel, E. W. *Transport Properties of Ions in Gases*; John Wiley & Sons: New York, 1988.
- Takagi, K.; Matsushima, F. Presented at the 15th Colloquium on High-Resolution Molecular Spectroscopy, Glasgow, Scotland, September 7–11, 1997; Abstract K27.
- Atkins, P. W. *Physical Chemistry*, 6th ed.; W. H. Freeman and Company: New York, 1998.
- Harris, D. C. *Quantitative Chemical Analysis*, 4th ed.; W. H. Freeman and Company: New York, 1995.
- Farley, J. W. *J. Chem. Phys.* **1991**, *95*, 5590.
- Civis, S. *Chem. Phys.* **1994**, *186*, 63.
- Woods, R. C.; Dixon, T. A.; Saykally, R. J.; Szanto, P. G. *Phys. Rev. Lett.* **1975**, *35*, 1269.
- Woods, R. C.; Saykally, R. J.; Anderson, T. G.; Dixon, T. A.; Szanto, P. G. *J. Chem. Phys.* **1981**, *75*, 4256.
- Haese, N. N.; Pan, F. S.; Oka, T. *Phys. Rev. Lett.* **1983**, *50*, 1575–1578.
- Picque, N.; Guelachvili, G. *Appl. Opt.* **1999**, *38*, 1224.
- Fan, W. Y.; Hamilton, P. A. *Chem. Phys. Lett.* **1994**, *230*, 555.
- Crofton, M. W.; Jagod, M. F.; Rehfuss, B. D.; Kreiner, W. A.; Oka, T. *J. Chem. Phys.* **1988**, *88*, 666.
- Gottfried, J. L.; McCall, B. J.; Oka, T. *J. Chem. Phys.* **2003**, *118*, 10890.
- Chen, G. L.; Yang, X. H.; Ying, X. P.; Liu, G.; Huang, Y. X.; Chen, Y. Q. *Chin. Sci. Bull.* **2004**, *49*, 2354.
- Darfus, J. D. www.wooster.edu/physics/JrIS/Files/Darfus-TheFaradayEffect.pdf, 1997.
- Bass, M. *Handbook of Optics*, 2nd ed.; McGraw-Hill: New York, 1995; Vol. 2, pp 36–45.
- Yu, S. S.; Y. X. H.; Li, B. X.; Kaniki, K.; Wu, S. H.; Guo, Y. C.; Liu, Y. Y.; Chen, Y. Q. *Chin. Phys.* **2003**, *12*, 745.
- Buckingham, A. D.; Stephens, P. J. *Annu. Rev. Phys. Chem.* **1996**, *17*, 399.
- Brown, J. M.; Buckingham, A. D.; Ramsey, D. A. *Can. J. Phys.* **1975**, *54*, 895.
- Brecha, R. J.; Pedrotti, L. M.; Krause, D. J. *Opt. Soc. Am. B* **1997**, *14*, 1921.
- Yang, X. H.; Chen, Y. Q.; Cai, P. P.; Wang, H.; Chen, J. H.; Xia, C. P. *Appl. Opt.* **1998**, *37*, 4806.
- Wu, S. H.; Chen, Y. Q.; Zhuang, H.; Yang, X. H.; Bi, Z.; Ma, L.; Lu, Y. Y. *J. Mol. Spectrosc.* **2001**, *209*, 133.
- Wu, L.; Yang, X.; Guo, Y.; Zheng, L.; Liu, Y.; Chen, Y. *J. Mol. Spectrosc.* **2005**, *230*, 72.
- Zhuang, H.; Yang, X. H.; Wu, S. H.; Bi, Z.; Ma, L.; Liu, Y. Y.; Chen, Y. Q. *Mol. Phys.* **2001**, *99*, 1447.
- Yang, X. H.; Chen, Y. Q.; Cai, P. P.; Wang, R. J.; Lu, J. J. *Acta Phys. Sin.* **2000**, *49*, 421.
- Zheng, L.; Yang, X. H.; Wu, L.; Kaniki, K.; Guo, Y.; Liu, Y. Y.; Chen, Y. Q. *J. Mol. Spectrosc.* **2004**, *226*, 81.
- Zheng, J.; Yang, X. H.; Wu, L.; Kaniki, K.; Guo, Y.; Liu, Y. Y.; Chen, Y. Q. *J. Mol. Spectrosc.* **2005**, *229*, 131.
- Gan, Y.; Yang, X. H.; Guo, Y. C.; Wu, S. H.; Li, W.; Liu, Y. Y.; Chen, Y. Q. *Mol. Phys.* **2004**, *102*, 611.
- Liu, Y.; Liu, H.; Gao, H.; Duan, C.; Hamilton, P. A.; Davies, P. B. *Chem. Phys. Lett.* **2000**, *317*, 181.
- Liu, Y. Y.; Gao, H.; Liu, H. P.; Duan, C. X.; Lin, J. L.; Guo, Y. Q.; Liu, X. Y.; Huang, G. M.; Li, J. R.; Li, F. Y. *Chin. Sci. Bull.* **2001**, *46*, 173.
- Liu, Y.; Duan, C.; Liu, J.; Wu, L.; Xu, C.; Chen, Y.; Hamilton, P. A.; Davies, P. B. *J. Chem. Phys.* **2002**, *116*, 9768.
- Duan, C.; Wu, L.; Chen, Y.; Liu, Y. *J. Mol. Spectrosc.* **2003**, *217*, 146.
- Liu, D. J.; Oka, T. *Phys. Rev. Lett.* **1985**, *54*, 1787.
- Evenson, K. M.; Jennings, D. A.; Peterson, F. R. *Appl. Phys. Lett.* **1984**, *44*, 576.
- Liu, Z. A.; Davies, P. B. *J. Chem. Phys.* **1997**, *107*, 337.
- Liu, D. J.; Ho, W. C.; Oka, T. *J. Chem. Phys.* **1987**, *87*, 2442.
- Purder, J.; Civis, S.; Blom, C. E.; VanHemert, M. C. *J. Mol. Spectrosc.* **1992**, *153*, 701.
- Crofton, M. W.; Altman, R. S.; Haese, N. N.; Oka, T. *J. Chem. Phys.* **1989**, *91*, 5882.
- Odashima, H.; Kozato, A.; Matsushima, F.; Tsunekawa, S.; Takagi, K. *J. Mol. Spectrosc.* **1999**, *195*, 356.
- Odishima, H.; Matsushima, F.; Kozato, A.; Tsunekawa, S.; Takagi, K.; Linnartz, H. *J. Mol. Spectrosc.* **1998**, *190*, 107.
- Filgueira, R. R.; Blom, C. E. *J. Mol. Spectrosc.* **1988**, *127*, 279.
- Brown, J. M.; Jennings, D. A.; Vanek, M.; Zink, L. R.; Evenson, K. M. *J. Mol. Spectrosc.* **1988**, *128*, 587.
- Asmis, K. R.; Pivonka, N. L.; Santambrogio, G.; Brummer, M.; Kaposta, C.; Neumark, D. M.; Woste, L. *Science* **2003**, *299*, 1375.
- Keutsch, F. N.; Saykally, R. J. *Proc. Natl. Acad. Sci. U.S.A.* **2001**, *98*, 10533.
- Fan, W. Y.; Hamilton, P. A. *Chem. Phys. Lett.* **1994**, *230*, 555.
- Davies, P. B.; Rothwell, W. J. *J. Chem. Phys.* **1985**, *83*, 5450.
- Amano, T. *J. Chem. Phys.* **1983**, *79*, 3595.
- Davies, P. B.; Rothwell, W. J. *J. Chem. Phys.* **1984**, *81*, 5239.
- Davies, P. B.; Hamilton, P. A.; Rothwell, W. J. *J. Chem. Phys.* **1984**, *81*, 1598.
- Liu, D. J.; Lee, S. T.; Oka, T. *J. Mol. Spectrosc.* **1988**, *128*, 236.
- Civis, S.; Blom, C. E.; Jensen, P. J. *J. Mol. Spectrosc.* **1989**, *138*, 69.
- Rosenbaum, N. H.; Owrutsky, J. C.; Tack, L. M.; Saykally, R. J. *J. Chem. Phys.* **1986**, *84*, 5308.
- Liu, D. J.; Oka, T. *J. Chem. Phys.* **1986**, *84*, 2426.

- (80) Rehfuss, B. D.; Crofton, M. W.; Oka, T. *J. Chem. Phys.* **1986**, *85*, 1785.
- (81) Tack, L. M.; Rosenbaum, N. H.; Owrutsky, J. C.; Saykally, R. J. *J. Chem. Phys.* **1986**, *85*, 4222.
- (82) Kawaguchi, K.; Hirota, E. *J. Chem. Phys.* **1987**, *87*, 6838.
- (83) Kawaguchi, K. *J. Chem. Phys.* **1988**, *88*, 4186.
- (84) Liu, Z.; Davies, P. B. *J. Chem. Phys.* **1996**, *105*, 3443.
- (85) Liu, Z.; Davies, P. B. *Phys. Rev. Lett.* **1996**, *76*, 596.
- (86) Lindsay, C. M.; McCall, B. J. *J. Mol. Spectrosc.* **2001**, *210*, 60.
- (87) Watson, J. K. G.; Foster, S. C.; MacKellar, A. R. W.; Bernath, P.; Amano, T.; Pan, F. S.; Crofton, M. W.; Altman, R. S.; Oka, T. *Can. J. Phys.* **1984**, *62*, 1875.
- (88) Lindsay, C. M.; Rade, R. M.; Oka, T. *J. Mol. Spectrosc.* **2001**, *210*, 51.
- (89) Xu, L. W.; Gabrys, C.; Oka, T. *J. Chem. Phys.* **1990**, *93*, 6210.
- (90) Lee, S. S.; Ventrudo, B. F.; Cassidy, D. T.; Oka, T.; Miller, S.; Tennyson, J. *J. Mol. Spectrosc.* **1991**, *145*, 222.
- (91) Ventrudo, B. F.; Cassidy, D. T.; Guo, Z. Y.; Joo, S. W.; Lee, S. S.; Oka, T. *J. Chem. Phys.* **1994**, *100*, 6263.
- (92) Uy, D.; Gabrys, C. M.; Jagod, M. F.; Oka, T. *J. Chem. Phys.* **1994**, *100*, 6267.
- (93) McCall, B. J.; Oka, T. *J. Chem. Phys.* **2000**, *113*, 3104.
- (94) Xu, L. W.; Rosslein, M.; Gabrys, C. M.; Oka, T. *J. Mol. Spectrosc.* **1992**, *153*, 726.
- (95) Lindsay, C. M.; White, E. T.; Oka, T. *Chem. Phys. Lett.* **2000**, *328*, 129.
- (96) Foster, S. C.; McKellar, A. R. W.; Peterkin, I. R.; Watson, J. K. G.; Pan, F. S.; Crofton, M. W.; Altman, R. S.; Oka, T. *J. Chem. Phys.* **1986**, *84*, 91.
- (97) Begemann, M. H.; Saykally, R. J. *J. Chem. Phys.* **1985**, *82*, 3570.
- (98) Begemann, M. H.; Gudeman, C. S.; Pfaff, J.; Saykally, R. J. *Phys. Rev. Lett.* **1983**, *51*, 554.
- (99) Haese, N. N.; Oka, T. *J. Chem. Phys.* **1984**, *80*, 572.
- (100) Liu, D. J.; Oka, T. *Phys. Rev. Lett.* **1985**, *54*, 1787.
- (101) Davies, P. B.; Hamilton, P. A.; Johnson, S. A. *J. Opt. Soc. Am. B-Opt. Phys.* **1985**, *2*, 794.
- (102) Davies, P. B.; Hamilton, P. A.; Johnson, S. A. *Astron. Astrophys.* **1984**, *141*, L9.
- (103) Tang, J.; Oka, T. *J. Mol. Spectrosc.* **1999**, *196*, 120.
- (104) Uy, D.; White, E. T.; Oka, T. *J. Mol. Spectrosc.* **1997**, *183*, 240.
- (105) Ho, W. C.; Ozier, I.; Cramb, D. T.; Gerry, M. C. L. *J. Mol. Spectrosc.* **1991**, *149*, 530.
- (106) Stahn, A.; Solka, H.; Adams, H.; Urban, W. *Mol. Phys.* **1987**, *60*, 121.
- (107) Haese, N. N.; Oka, T. *J. Mol. Spectrosc.* **1988**, *130*, 262.
- (108) Crofton, M. W.; Altman, R. S.; Jagod, M. F.; Oka, T. *J. Phys. Chem.* **1985**, *89*, 3614.
- (109) Rehfuss, B. D.; Jagod, M. F.; Xu, L. W.; Oka, T. *J. Mol. Spectrosc.* **1992**, *151*, 59.
- (110) Dinelli, B. M.; Crofton, M. W.; Oka, T. *J. Mol. Spectrosc.* **1988**, *127*, 1.
- (111) Brown, P. R.; Davies, P. B.; Stickland, R. J. *J. Chem. Phys.* **1989**, *91*, 3384.
- (112) Huet, T. R.; Pursell, D. C.; Ho, W. C.; Dinelli, B. M.; Oka, T. *J. Chem. Phys.* **1992**, *97*, 5977.
- (113) Das, B.; Farley, J. W. *J. Chem. Phys.* **1991**, *95*, 8809.
- (114) Huet, T. R.; Bachir, I. H.; Destombes, J. L.; Vervloet, M. *J. Chem. Phys.* **1997**, *107*, 5645.
- (115) Wu, S.; Yang, X.; Guo, Y.; Zhuang, H.; Liu, Y.; Chen, Y. *J. Mol. Spectrosc.* **2003**, *219*, 258.
- (116) Tarsitano, C. G.; Oka, T. *J. Mol. Spectrosc.* **2003**, *219*, 263.
- (117) Bachir, I. H.; Huet, T. R.; Destombes, J. L. *J. Mol. Spectrosc.* **1995**, *170*, 601.
- (118) Ho, W. C.; Jager, W.; Cramb, D. T.; Ozier, I.; Gerry, M. C. L. *J. Mol. Spectrosc.* **1992**, *153*, 692.
- (119) Collet, D.; Huet, T. R. *J. Mol. Spectrosc.* **1999**, *197*, 46.
- (120) Collet, D.; Destombes, J. L.; Bachir, I. H.; Huet, T. R. *Chem. Phys. Lett.* **1998**, *286*, 311.
- (121) Okumura, M.; Rehfuss, B. D.; Dinelli, B. M.; Bawendi, M. G.; Oka, T. *J. Chem. Phys.* **1989**, *90*, 5918.
- (122) Kabbadj, Y.; Huet, T. R.; Uy, D.; Oka, T. *J. Mol. Spectrosc.* **1996**, *175*, 277.
- (123) Kabbadj, Y.; Huet, T. R.; Rehfuss, B. D.; Gabrys, C. M.; Oka, T. *J. Mol. Spectrosc.* **1994**, *163*, 180.
- (124) Owrutsky, J. C.; Gudeman, C. S.; Martner, C. C.; Tack, L. M.; Rosenbaum, N. H.; Saykally, R. J. *J. Chem. Phys.* **1986**, *84*, 605.
- (125) Nesbitt, D. J.; Petek, H.; Gudeman, C. S.; Moore, C. B.; Saykally, R. J. *J. Chem. Phys.* **1984**, *81*, 5281.
- (126) Huet, T. R.; Kabbadj, Y.; Gabrys, C. M.; Oka, T. *J. Mol. Spectrosc.* **1994**, *163*, 206.
- (127) Bawendi, M. G.; Rehfuss, B. D.; Dinelli, B. M.; Okumura, M.; Oka, T. *J. Chem. Phys.* **1989**, *90*, 5910.
- (128) Lee, S. S.; Oka, T. *J. Chem. Phys.* **1991**, *94*, 1698.
- (129) Crofton, M. W.; Oka, T. *J. Chem. Phys.* **1987**, *86*, 5983.
- (130) Schafer, E.; Saykally, R. J.; Robiette, A. G. *J. Chem. Phys.* **1984**, *80*, 3969.
- (131) Crofton, M. W.; Oka, T. *J. Chem. Phys.* **1983**, *79*, 3157.
- (132) Schafer, E.; Saykally, R. J.; Robiette, A. G. *J. Chem. Phys.* **1984**, *80*, 3969.
- (133) Ho, W. C.; Ozier, I.; Cramb, D. T.; Gerry, M. C. L. *J. Mol. Spectrosc.* **1991**, *149*, 559.
- (134) Anicich, V. G.; McEwan, M. J. *Icarus* **2001**, *154*, 522.
- (135) Ho, W. C.; Blom, C. E.; Liu, D. J.; Oka, T. *J. Mol. Spectrosc.* **1987**, *123*, 251.
- (136) Liu, D. J.; Lee, S. T.; Oka, T. *J. Mol. Spectrosc.* **1988**, *128*, 236.
- (137) Altman, R. S.; Crofton, M. W.; Oka, T. *J. Chem. Phys.* **1984**, *81*, 4255.
- (138) Altman, R. S.; Crofton, M. W.; Oka, T. *J. Chem. Phys.* **1984**, *80*, 3911.
- (139) White, E. T.; Tang, J.; Oka, T. *Science* **1999**, *284*, 135.
- (140) Rehfuss, B. D.; Liu, D. J.; Dinelli, B. M.; Jagod, M. F.; Ho, W. C.; Crofton, M. W.; Oka, T. *J. Chem. Phys.* **1988**, *88*, 129.
- (141) Taristano, C. G.; Neese, C. F.; Oka, T. *J. Chem. Phys.* **2004**, *121*, 6290.
- (142) Jagod, M. F.; Gabrys, C. M.; Rosslein, M.; Uy, D.; Oka, T. *Can. J. Phys.* **1994**, *72*, 1192.
- (143) Crofton, M. W.; Altman, R. S.; Jagod, M. F.; Oka, T. *J. Chem. Phys.* **1985**, *83*, 3702.
- (144) Rosslein, M.; Jagod, M. F.; Gabrys, C. M.; Oka, T. *Astrophys. J.* **1991**, *382*, L51.
- (145) Jagod, M. F.; Rosslein, M.; Gabrys, C. M.; Oka, T. *J. Mol. Spectrosc.* **1992**, *153*, 666.
- (146) Jagod, M. F.; Rosslein, M.; Gabrys, C. M.; Rehfuss, B. D.; Scappini, F.; Crofton, M. W.; Oka, T. *J. Chem. Phys.* **1992**, *97*, 7111.
- (147) Crofton, M. W.; Jagod, M. F.; Rehfuss, B. D.; Oka, T. *J. Chem. Phys.* **1987**, *86*, 3755.
- (148) Crofton, M. W.; Jagod, M. F.; Rehfuss, B. D.; Oka, T. *J. Chem. Phys.* **1989**, *91*, 5139.
- (149) Davies, P. B.; Hamilton, P. A.; Johnson, S. A. *Mol. Phys.* **1986**, *57*, 217.
- (150) Chanda, A.; Ho, W. C.; Dalby, F. W.; Ozier, I. *J. Mol. Spectrosc.* **1995**, *169*, 108.
- (151) Chanda, A.; Ho, W. C.; Ozier, I. *J. Chem. Phys.* **1995**, *102*, 8725.
- (152) Schafer, E.; Saykally, R. J. *J. Chem. Phys.* **1984**, *81*, 4189.
- (153) Schafer, E.; Saykally, R. J. *J. Chem. Phys.* **1984**, *80*, 2973.
- (154) Hunt, N. T.; Collet, D.; Liu, Z.; Davies, P. B. *J. Chem. Phys.* **1999**, *111*, 5905.
- (155) Hunt, N. T.; Liu, Z.; Davies, P. B. *Mol. Phys.* **1999**, *97*, 205.
- (156) Gruebele, M.; Polak, M.; Saykally, R. J. *J. Chem. Phys.* **1986**, *85*, 6276.
- (157) Fan, W. Y.; Liu, Z.; Davies, P. B. *J. Mol. Spectrosc.* **1998**, *191*, 98.
- (158) Gruebele, M.; Polak, M.; Saykally, R. J. *J. Chem. Phys. Lett.* **1986**, *125*, 165.
- (159) Focsa, C.; Pinchemel, B.; Femenias, J. L.; Huet, T. R. *J. Chem. Phys.* **1997**, *107*, 10365.
- (160) Kaledin, L. A.; Heaven, M. C. *J. Chem. Phys.* **1997**, *107*, 7020.
- (161) Focsa, C.; Dufour, C.; Pinchemel, B.; Bachir, I. H.; Huet, T. R. *J. Chem. Phys.* **1997**, *106*, 9044.
- (162) Focsa, C.; Pinchemel, B.; Collet, D.; Huet, T. R. *J. Mol. Spectrosc.* **1998**, *189*, 254.
- (163) Focsa, C.; Pinchemel, B. *Chem. Phys.* **1999**, *247*, 395.
- (164) Davies, P. B.; Martineau, P. M. *J. Chem. Phys.* **1988**, *88*, 485.
- (165) Davies, P. B.; Smith, D. M. *J. Chem. Phys.* **1994**, *100*, 6166.
- (166) Smith, D. M.; Martineau, P. M.; Davies, P. B. *J. Chem. Phys.* **1992**, *96*, 1741.
- (167) Rosenbaum, N. H.; Owrutsky, J. C.; Tack, L. M.; Saykally, R. J. *J. Chem. Phys.* **1985**, *83*, 4845.

CR040100D

